

# Decline and poleward shift in Indian summer monsoon synoptic activity in a warming climate

S. Sandeep<sup>a,b</sup>, R. S. Ajayamohan<sup>a,1</sup>, William R. Boos<sup>c,d</sup>, T. P. Sabin<sup>a,e</sup>, and V. Praveen<sup>a</sup>

<sup>a</sup>The Center for Prototype Climate Modeling, New York University Abu Dhabi, Abu Dhabi, United Arab Emirates; <sup>b</sup>Centre for Atmospheric Sciences, Indian Institute of Technology Delhi, New Delhi 110016, India; <sup>c</sup>Department of Earth and Planetary Science, University of California, Berkeley, CA 94720; <sup>d</sup>Climate and Ecosystem Sciences Division, Lawrence Berkeley National Laboratory, Berkeley, CA 94720; and <sup>e</sup>Center for Climate Change Research, Indian Institute of Tropical Meteorology, Pune, Maharashtra 411008, India

Edited by John M. Wallace, University of Washington, Seattle, WA, and approved January 24, 2018 (received for review May 31, 2017)

Cyclonic atmospheric vortices of varying intensity, collectively known as low-pressure systems (LPS), travel northwest across central India and produce more than half of the precipitation received by that fertile region and its ~600 million inhabitants. Yet, future changes in LPS activity are poorly understood, due in part to inadequate representation of these storms in current climate models. Using a high-resolution atmospheric general circulation model that realistically simulates the genesis distribution of LPS, here we show that Indian monsoon LPS activity declines about 45% by the late 21st century in simulations of a business-as-usual emission scenario. The distribution of LPS genesis shifts poleward as it weakens, with oceanic genesis decreasing by ~60% and continental genesis increasing by ~10%; over land the increase in storm counts is accompanied by a shift toward lower storm wind speeds. The weakening and poleward shift of the genesis distribution in a warmer climate are confirmed and attributed, via a statistical model, to the reduction and poleward shift of low-level absolute vorticity over the monsoon region, which in turn are robust features of most coupled model projections. The poleward shift in LPS activity results in an increased frequency of extreme precipitation events over northern India.

monsoon | low-pressure systems | climate change | precipitation extremes

**A**lthough precipitating atmospheric vortices known as low-pressure systems (LPS) are found in all monsoon regions, their presence is most prominent over India, where an average of 13 ( $\pm 2.5$ ) storms develop each boreal summer, with most originating over the Bay of Bengal (BoB) and adjoining land (1–5). The intensification and propagation of these storms are linked to the strength of the larger-scale monsoon circulation and interactions with precipitating convection (6, 7). The mean monsoon circulation is argued to have weakened in recent decades, with a variety of reasons advanced for this slowdown of winds (8, 9). Some studies have also reported a reduction in LPS activity since the mid-20th century (10–12), but the reliability of this trend has been questioned due to inconsistencies among observational datasets (13).

A lack of understanding of the mechanism of LPS development has hindered projections of future monsoon synoptic activity, leaving us reliant on simulations of future scenarios by comprehensive climate models. However, the unrealistic representation of these systems in global climate models (GCMs) used in the fifth phase of the Coupled Model Intercomparison Project (CMIP5; ref. 14) is an obstacle to the reliable estimation of future LPS activity (4). Similar issues in estimating future changes in global tropical cyclone (TC) activity were addressed using a high-resolution atmospheric GCM; the same high-resolution modeling strategy was also found reliable in simulating the distribution and structure of Indian monsoon LPS (15, 16). Here we use that high-resolution atmospheric GCM, together with a statistical model, to project and understand possible trends in LPS activity over the next century.

## Monsoon Synoptic Activity in Current and Future Climates

Two sets of numerical experiments are performed here using the High Resolution Atmospheric Model (HiRAM; ref. 15) with a horizontal grid spacing of 50 km globally. One set of simulations represents the historical (HIST) period and the other a late-21st-century climate scenario based on the strongest Representative Concentration Pathway (RCP8.5). Four ensemble members of these simulations are run, with sea surface temperatures (SSTs) taken from different CMIP5 GCMs selected for their skill in simulating the Indian monsoon. In addition, 30 ensemble members of annual cycle (ANNC) experiments are run for each of the HIST and RCP8.5 scenarios to assess model uncertainty, in which the model is forced with ANNCs of decadal mean SSTs (*Materials and Methods*).

HiRAM simulates a realistic mean monsoon circulation, precipitation, and LPS frequency compared with most CMIP5 models (*SI Appendix, Figs. S1–S4*). The SAI (17), a combined measure of the frequency, intensity, and duration of LPS, shows a strong and well-defined pattern over the monsoon trough region in the HIST ensemble (Fig. 14). The horizontal structure of the SAI in HIRAM compares well with observations (Sikka archive, 1979–2003 period; ref. 18), albeit with an overestimation of the amplitude of the SAI distribution associated with the distribution of storm intensity's being biased toward stronger systems (*SI Appendix, Fig. S4*). The number of LPS simulated by HIRAM matches observations better than any other CMIP5 model.

## Significance

Propagating atmospheric vortices contribute more than half of the total rainfall received by the fertile and highly populated Gangetic plains of India. How the activity of these storms will change in a warming climate is not yet understood, due to both the inadequate representation of these disturbances in global climate models and a lack of theory for their fundamental dynamics. Here we show that both a high-resolution atmospheric model and a statistical model predict that the activity of these storms weakens and shifts poleward from ocean to land in a warmer environment. The associated changes in seasonal mean rainfall and precipitation extremes are expected to have serious implications for the hydrological cycle of South Asia.

Author contributions: S.S., R.S.A., and T.P.S. designed research; S.S., T.P.S., and V.P. performed research; W.R.B. and V.P. contributed new reagents/analytic tools; S.S. analyzed data; and S.S., R.S.A., and W.R.B. wrote the paper.

The authors declare no conflict of interest.

This article is a PNAS Direct Submission.

This open access article is distributed under Creative Commons Attribution-NonCommercial-NoDerivatives License 4.0 (CC BY-NC-ND).

<sup>1</sup>To whom correspondence should be addressed. Email: Ajaya.Mohan@nyu.edu.

This article contains supporting information online at [www.pnas.org/lookup/suppl/doi:10.1073/pnas.1709031115/-DCSupplemental](http://www.pnas.org/lookup/suppl/doi:10.1073/pnas.1709031115/-DCSupplemental).

Published online February 26, 2018.

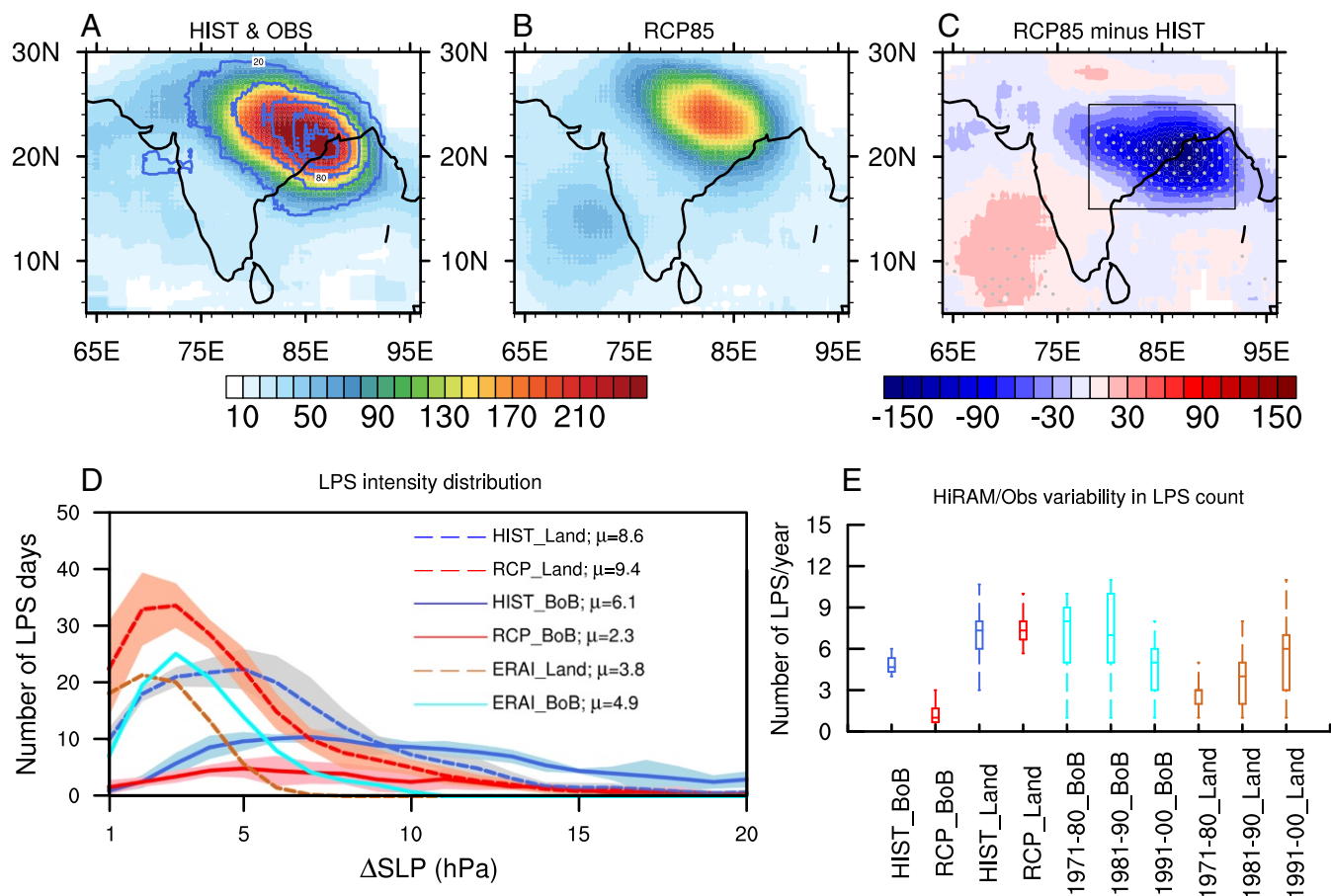


**Fig. 1.** June–September ensemble mean climatology of Synoptic Activity Index (SAI) from (A) HIST (shaded) and the 1979–2003 Sikka archive (blue contours, ranging from 20 to 140 with an interval of 30), (B) RCP8.5 ensembles, and (C) difference in SAI climatology between RCP8.5 and HIST, where the stippling represents the changes in SAI that are statistically significant at the 5% level for each ensemble, as revealed by a *t* test. The area averaged difference in the mean of SAI between RCP8.5 and HIST over the box in C is 45%. (D) Frequency distribution of sea-level pressure depth of LPS from ERAI (interim version of European center reanalysis) and HIST and RCP8.5 simulations of HiRAM. Solid (dashed) lines represent systems that form over the BoB (Indian land region). Lines (shading) show ensemble mean (spread) for HiRAM HIST and RCP8.5 experiments. The future change in mean of  $\Delta SLP$  distribution for LPS over BoB is statistically significant ( $P < 0.01$ ), as revealed by a Kolmogorov–Smirnov test. Note that the future change in mean  $\Delta SLP$  distribution for LPS over land region is not statistically significant. (E) The model spread in the annual LPS count for HIST and RCP8.5 simulations from the ANNC experiments forced with decadal mean SST ANNCs, and the observed decadal variability in LPS counts over BoB and land for the decades of 1971–1980, 1981–1990, and 1991–2000, based on the Sikka archive.

The future projections show a strong weakening of LPS activity in the main genesis region over the BoB and over land immediately to the northwest (Fig. 1 *B* and *C*). The coarse-resolution CMIP5 model ensemble also shows a weakening of synoptic activity over central India in the RCP8.5 simulations (*SI Appendix, Fig. S3*), but the poor representation of LPS structure in those models raised questions about their validity for use in projections.

the Sikka dataset (18) also decreases over the BoB and increases over land in the last three decades of the 20th century, but these trends are modest compared with interannual variability within each decade (Fig. 1E; *SI Appendix*, Fig. S5 shows a similar analysis of individual decades in HiRAM). The climatological difference in the Sikka-based SAI between the last two quarters of the 20th century also shows increased LPS activity over many land regions, but the BoB changes are more modest and inhomogeneous in sign (*SI Appendix*, Fig. S3 G and H). Trends in LPS counts and SAI in the HiRAM projections rise above the level of internal variability much more than observed (Fig. 1E) or simulated (*SI Appendix*, Fig. S5) changes in recent decades; these ensemble means of the HIST and RCP8.5 simulations are not expected to be influenced by internal decadal variability because the SST boundary conditions are drawn from 10 different CMIP5 coupled models.

Observations suggest that genesis frequency over land is less than that over ocean, with about 139 and 176 storms formed over continental India and the BoB, respectively, during 1979–2003. Although HiRAM simulates nearly the same total number of LPS as observed, it produces more frequent genesis over land ( $180 \pm 19$ ) than ocean ( $128 \pm 14$ ) during the 25 y of the historical

lated by HiRAM—but much of the MDGI increase is along the foothills of the Himalaya where genesis would likely be inhibited by orography.

**Statistical Projection of Synoptic Activity.** These changes in genesis frequency can be understood using an existing statistical model of the observed spatial distribution and seasonal cycle of global LPS genesis. That model, the MDGI (19), predicts the likelihood of genesis from monthly mean climatologies of precipitable water (PW), low-level absolute vorticity ( $\eta$ ), an estimate of convective available potential energy (CAPE), and midtropospheric relative humidity (RH). These four variables were objectively selected using observed LPS counts, but when the MDGI is calculated using the same four climatological variables from HiRAM it also successfully represents the distribution of LPS genesis explicitly simulated in HIST (Fig. 2C). Furthermore, the MDGI predicts a strong reduction of genesis frequency over the BoB in the future (Fig. 2D). That is, given only the simulated change in the climatological monthly mean state, the MDGI predicts a roughly 50% decrease in genesis frequency over the BoB. It also predicts a roughly 50% increase in genesis over land—much larger than the increase in LPS genesis explicitly simu-

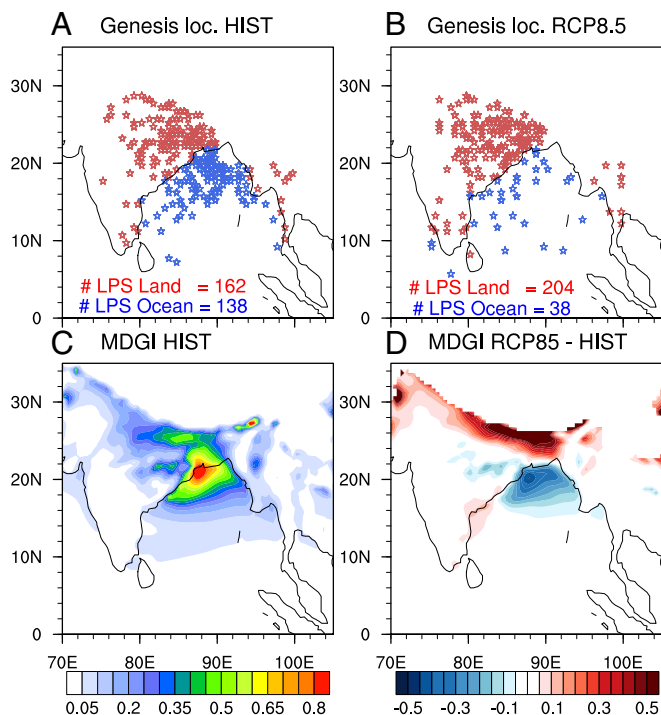
### Mechanisms of Weakening of Synoptic Activity

The MDGI is based on a log-linear model, so its changes can be linearly attributed to changes in its constituent environmental variables. Most of the MDGI change is produced by a reduction and poleward shift in the low-level absolute vorticity,  $\eta$ . The HIST climatology of  $\eta$  is maximum over the core LPS genesis area due mostly to shear vorticity of the low-level monsoon westerlies, and this maximum weakens and shifts poleward in the RCP8.5 projection, producing a nearly 100% decrease and a poleward shift in the component of the MDGI associated with  $\eta$  (Fig. 3). The changes in PW and RH make small contributions to the MDGI change, while an increase in ECAPE strengthens the MDGI everywhere, especially over India's east coast and around Pakistan, offsetting some of the reduction due to  $\eta$  (*SI Appendix, Fig. S7*).

This suggests that the large reduction in future LPS genesis simulated by HiRAM is caused by a weakening of the large-scale monsoon circulation and a corresponding drop in the ambient vorticity from which LPS form. Although the genesis mechanism of LPS is still the subject of active research (20), the presence of large low-level vorticity has been long held to be essential for genesis (21). Recently, monsoon LPS have also been shown to have structural similarities to weak TCs (20) and to have a statistical association with the climatological mean state similar to that of TCs (19), which suggests that LPS genesis may also be favored by environments rich in cyclonic vorticity. This reasoning contrasts with a previous argument relating the possible recent decline in LPS activity to a midtropospheric drying (12); HiRAM simulates such a drying, but it produces a comparatively minor effect on the MDGI (*SI Appendix, Fig. S7*). The projected weakening of  $\eta$  in HiRAM is in broad agreement with that in the CMIP5 ensemble mean, although the HiRAM weakening is stronger (*SI Appendix, Fig. S7*). Weakening of the large-scale monsoon circulation over the last half-century has also been observed, although its underlying cause is debated (8, 9, 22). A slowing of tropical circulations in general may be expected from the increase in static stability that occurs in a warming troposphere (23), but the degree to which changes in diabatic heating might compensate in monsoon circulations is unclear.

In summary, the hypothesis that future LPS genesis will decrease in frequency over the BoB is supported by numerous future projections of a weakening of the large-scale monsoon circulation and by a statistical model that links the large-scale circulation strength to LPS genesis frequency; in addition, HiRAM explicitly simulates a reduction in LPS genesis frequency for all four SST forcings. It has been argued that monsoon LPS over the BoB may result from the amplification of disturbances originating over the West Pacific (24, 25), which might link LPS frequency to the distribution of West Pacific storms, but those studies were based on relatively small samples of LPS. Automated tracking of low-level 850-hPa vorticity anomalies has not found a large number of BoB LPS to originate from the West Pacific (5), so we leave investigation of the connection between the monsoon LPS and West Pacific disturbances in a warming climate for future work.

The projected reduction in synoptic activity is due not only to reduced genesis frequency but also to the general decrease in LPS intensity (Fig. 1D). We now discuss possible reasons for this intensity decrease. Although the mechanism of LPS intensification is not understood, LPS have multiple dynamical similarities to weak TCs (20), which have been projected to decrease in number in a warming climate (26). Those projections of TC counts typically only consider storms with sustained surface wind speeds of  $20 \text{ m s}^{-1}$  or greater (26, 27), which is stronger than





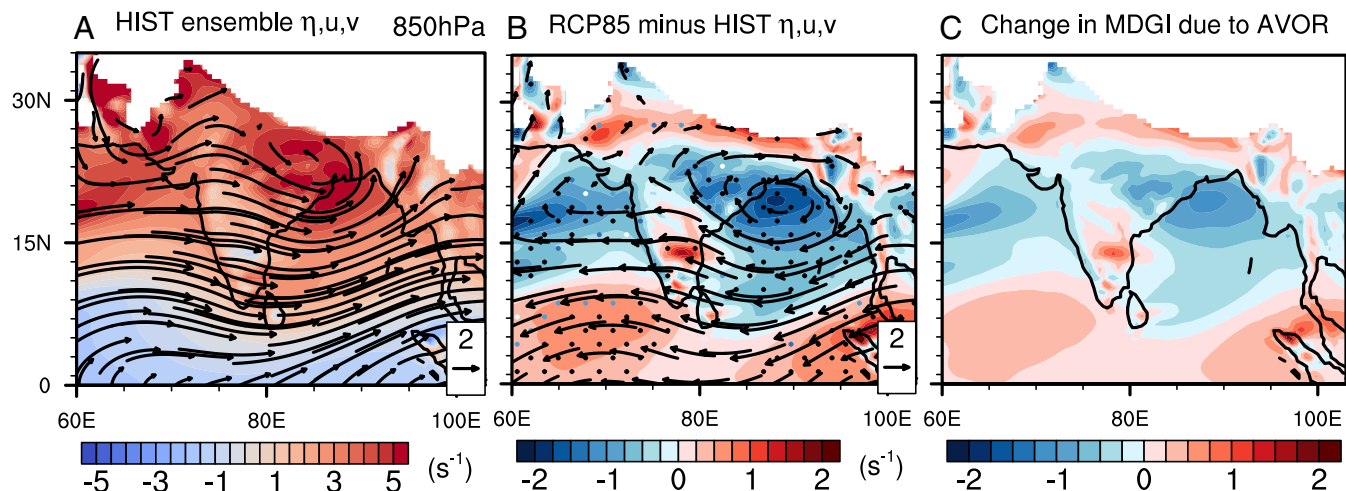


**Fig. 3.** June–September ensemble mean climatology of 850-hPa wind (vectors,  $\text{m s}^{-1}$ ) and absolute vorticity (shaded) from (A) HIST. (B) Difference between RCP8.5 and HIST simulations. (C) Difference in MDGI due to absolute vorticity between RCP8.5 and HIST simulations. All based on HiRAM. Stippling in B represents statistically significant (at 5% level) changes in absolute vorticity for all ensemble members.

nearly all Indian summer monsoon LPS; a general reduction in LPS intensity is thus consistent with projections of reduced TC counts, as fewer LPS achieve sufficient intensities to be counted as TCs. The reduction of TC frequency has been attributed to an increase in the midtropospheric saturation deficit (27) (amount of moisture needed to achieve saturation) and to a weakening of the large-scale tropical circulation, both of which are simulated to occur in the HiRAM future projections (*SI Appendix, Figs. S8 and S9*). In the HiRAM projections, the troposphere over the BoB and central India exhibits a stronger increase in saturation deficit than that over the equatorial Indian Ocean, possibly causing a reduction in LPS intensity by strengthening unsaturated convective downdrafts and weakening the upward convective mass flux in those storms.

#### Influence of Changes in Synoptic Activity on Precipitation

A change in LPS activity is expected to alter the distribution of monsoon precipitation. The climatological precipitation is strong over the BoB and into central India along the typical LPS trajectory (Fig. 4A). The climatology of precipitation related to LPS originating in the BoB shows that those storms contribute to both continental and oceanic rainfall (Fig. 4B). The LPS originating over land contribute more to continental rainfall, especially in the northern parts of India (Fig. 4C). These patterns of LPS-related rainfall illustrate the importance of these storms for the hydrology of India and the Himalaya. The projected changes in seasonal mean rainfall show a significant drying over the BoB (Fig. 4A). The component of precipitation associated with the BoB storms declines substantially, consistent with the decrease in LPS genesis over the BoB (Fig. 4B). The contribution of LPS of continental origin to seasonal mean rainfall increases in the future projection (Fig. 4C).

These changes in synoptic activity have consequences not only for the mean precipitation but also for the extremes. Flooding over central and northern India is often associated with LPS activity (3, 28). Also, a recent increase in rainfall extremes over central India has been attributed to increased synoptic activity over that continental region (17, 29, 30). Fig. 4D shows the climatology and the difference between RCP8.5 and HIST simulations of the 95th percentile of daily precipitation over the Indian region. The nonorographic precipitation extremes occur most frequently slightly south of the peak swath of synoptic activity (Figs. 1A and 2A and C), consistent with the fact that the peak precipitation in LPS typically occurs southwest of the vortex cen-

ter (1). The future changes in precipitation extremes over India reflect the changes in LPS activity, with a poleward shift clearly evident in the 95th percentile of precipitation (compare Figs. 4D and 2B and D). One caveat is that GCMs with parameterized convection typically do not simulate extreme precipitation accurately, so such projections should be treated with caution. Also, we lack a long-term record of observed rainfall over the BoB that

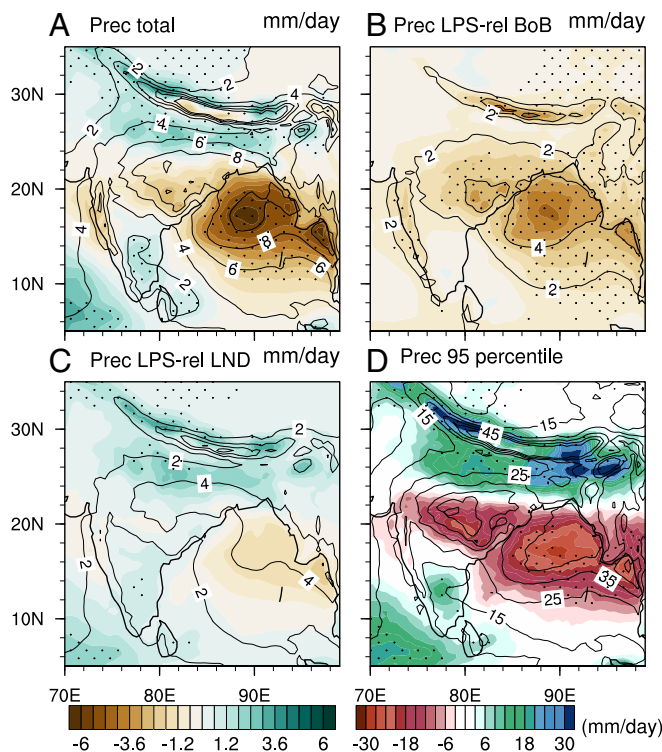


**Fig. 4.** June–September ensemble mean HIST climatology (contours) and RCP8.5 minus HIST climatology (shading) of (A) total seasonal mean precipitation, (B) BoB LPS-related precipitation, (C) land-based LPS-related precipitation, and (D) 95th-percentile precipitation, all based on HiRAM. Stippling represents the changes that are statistically significant (at 5% level) for all ensemble members. The color bar at the bottom left corresponds to A–C.

could be used to assess the fidelity of historical model simulations in that oceanic region.

Furthermore, the northward shift of the genesis distribution may reduce the amount of warning India has for flood events. In the HiRAM HIST simulations it takes about 3.7 d for an LPS to make landfall after its genesis over the BoB. This time between genesis and landfall is helpful in preparing mitigation strategies for impending floods. As the LPS genesis shifts from ocean to land the Indian region may face shorter preparation times for mitigating the societal impacts of these storms.

## Summary and Discussion

Despite the importance of monsoon LPS, future changes in these systems remain poorly characterized and incompletely understood. We have shown that one of the few GCMs to successfully simulate the genesis distribution of Indian monsoon LPS projects a strong weakening and poleward shift of LPS activity in a warming environment. This occurs for all four ensemble members, despite their differing SSTs. An existing statistical model that successfully reproduces the observed global distribution of LPS also predicts a decrease in LPS genesis and furthermore attributes this decrease to a weakening and poleward shift of the large-scale monsoon flow that is widespread in CMIP5 projections. This important consequence of the weakening and poleward shift of the low-level monsoon flow has not been previously appreciated.

The poleward shift in LPS activity was shown to be associated with increased precipitation extremes over northern India in HiRAM. Given the poor skill with which most other climate models simulate LPS activity and associated precipitation, the HiRAM projections may have greater relevance for future changes in regional monsoon climates (31–33). Whether the positive bias in the intensity of LPS simulated by HiRAM compromises the validity of these projections remains unclear, but this bias in LPS properties is substantially smaller than the LPS biases seen in nearly all other CMIP5 models (4). Central and northern India are some of the most intensively irrigated regions worldwide and have water resources that are already stressed (34) and growing populations that are highly vulnerable to hydrological extremes (35). A shift in synoptic activity that dries central India and increases the likelihood of extreme rainfall in northern India (e.g., Fig. 4) would have major societal impact.

## Materials and Methods

Monthly varying SSTs from four climate models (Community Climate System Model 4, GFDL-CM3, GFDL-Earth System Model 2G, and Model for Interdisciplinary Research on Climate 5) participating in CMIP5 are used to force the HiRAM model. These models are chosen based on two criteria: (i) their skill in simulating June–September seasonal mean monsoon precipitation over India (22) and (ii) the SST bias over the Arabian Sea, which is found to introduce a dry bias over India (36, 37) (models with weaker bias are preferred). Biases in climate model SSTs can lead to errors when atmospheric models are forced with these SSTs (38). Hence, we applied an SST bias correction (described below). The HiRAM model is configured with a horizontal resolution of 50 km and 32 vertical hybrid pressure levels.

The SST from GCM ( $SST_M$ ) can be decomposed into monthly climatological mean in the present climate ( $\overline{SST_M}$ ) and anomaly ( $SST'_M$ ) as

$$SST_M = \overline{SST_M} + SST'_M.$$

The observed SSTs ( $SST_O$ ) can also be decomposed and written as anomalies about a present-day climatological mean:

$$SST_O = \overline{SST_O} + SST'_O.$$

Here we used Hadley Center Sea Ice and Sea Surface Temperatures (HadISST1.1; ref. 39). We assume that the bias in the mean SST field of the model. The bias-corrected SST ( $SST_B$ ) is obtained by adding the model anomalies to the observed climatology:

$$SST_B = \overline{SST_O} + SST'_M.$$

The SST anomalies from RCP8.5 simulations are added to the observed climatology to get bias-corrected future SST fields. The observed climatology is calculated for 1979–2005. Variability in the SSTs is characterized in *SI Appendix, Fig. S10* and discussed in the *SI Appendix, Supporting Methods*. Two types of experiments (transient time slice and ANNC) are performed using HiRAM, as follows.

### Time-Slice Simulations.

**Historical time-slice experiment (HIST).** In this experiment, the HiRAM model is forced with bias-corrected SSTs for the period 1979–2005. In addition to the SST and sea ice concentrations (SIC) from the CMIP5 coupled models, the standard CMIP5 forcings such as monthly varying greenhouse gases, solar irradiance, aerosol, ozone, and so on are used to drive the model. An ensemble of four simulations is produced, with each simulation corresponding to the SST and SIC from a CMIP5 coupled model.

**Late-21st-century time-slice experiment (RCP8.5).** Bias-corrected future SSTs from the four CMIP5 models along with other CMIP5 atmospheric forcings for RCP8.5 are used to drive the HiRAM model to simulate four ensemble members for the 2069–2095 period. To avoid analyzing the model spin-up period the analyses are restricted to 1981–2005 and 2071–2095 for HIST and RCP8.5, respectively.

**ANNC Simulations.** Since performing this ensemble of HiRAM simulations is computationally intensive, another set of experiments is run in ANNC mode to quantify model uncertainty. These simulations are forced with ANNCs of 10-y mean SSTs and other model forcings. SSTs from 10 different CMIP5 coupled models (historical and RCP8.5 experiments; see *SI Appendix, Supporting Methods*) are used for these simulations. Three sets of ANNC simulations are carried out with each coupled model SST, where the SST ANNCs correspond to the decades 1971–1980, 1981–1990, and 1991–2000 for the HIST and the decades 2071–2080, 2081–2090, and 2091–2100 for the RCP8.5 scenario. In these experiments HiRAM is integrated for 24 mo, with the first 12 mo treated as a spin-up period.

**LPS Tracking.** LPS tracks from HiRAM simulations and reanalysis data are extracted using a tracking algorithm that mimics the conventional detection and tracking of LPS by identifying closed isobars (4). The LPS activity from HIST simulations are compared with those from ERA-Interim reanalysis as well as from the Sikka archive. See *SI Appendix, Supporting Methods* for details of the LPS tracking algorithm. The storm intensity is measured by the maximum pressure depth ( $\Delta SLP$ ) achieved by the storm during its life cycle.  $\Delta SLP$  is defined as the difference between the value of outermost closed isobar and the central minimum pressure of the storm. It is also to be noted that here we only consider storms that lasted 3 d or more. The LPS activity is quantitatively represented by an SAI which is track density-weighted by wind speed (17) as

$$SAI_{xy} = \sum_{x-\Delta x}^{x+\Delta x} \sum_{y-\Delta y}^{y+\Delta y} U_{cat},$$

where  $x$  and  $y$  are the longitude and latitude of the center of LPS,  $\Delta x = \Delta y = 1.5^\circ$ , and  $U_{cat}$  is the wind speed magnitude based on the intensity category of the LPS. The values of  $U_{cat}$  are 4.25, 11, 15, 20, and 27.5, respectively, for LPS categories of Low (1 hPa <  $\Delta SLP \leq 2$  hPa), Depression (2 hPa <  $\Delta SLP \leq 4$  hPa), Deep Depression (4 hPa <  $\Delta SLP \leq 10$  hPa), Cyclonic Storm (10 hPa <  $\Delta SLP \leq 16$  hPa), and Severe Cyclonic Storm ( $\Delta SLP > 16$  hPa).

**MDGI.** The MDGI is a statistical model that predicts the likelihood of LPS genesis as a function of climatological monthly mean variables (19). The expected number of LPS genesis points  $\mu$  is written as a log-linear model,

$$\mu = \exp[\mathbf{b}^T \mathbf{x} + \log(\Delta x \Delta y T \cos \phi)],$$

where  $\mathbf{b}$  is a vector of coefficients multiplying the climatological variables in the vector  $\mathbf{x}$ ,  $\Delta x$  and  $\Delta y$  are the longitude and latitude grid spacing, respectively,  $T$  is the number of years in the storm count record, and  $\phi$  is latitude. The variables in  $\mathbf{x}$  were objectively selected in the original MDGI using cross-validation to avoid overfitting. The functional form of the MDGI permits fractional changes in genesis frequency to be expressed as a linear function of changes in the climatological variables,

$$\frac{\delta\mu}{\mu} = \mathbf{b}^T \mathbf{x}.$$

Using Poisson regression we refit the log-linear model to HiRAM storm counts in the HIST simulations for June–September, giving one set of MDGI coefficients for each of the four ensemble members. All four sets of coefficients were similar to each other and to the previously derived coefficients obtained using global observations of LPS counts for the full calendar year (19), but the HiRAM coefficients had larger standard errors due to the smaller number of storms occurring in the Indian region.

**ACKNOWLEDGMENTS.** The Center for Prototype Climate Modeling is fully funded by the Government of Abu Dhabi through a New York University Abu Dhabi Research Institute grant. This work was supported by a Monsoon Mission grant from the Ministry of Earth Sciences, Government of India (Grant MM/SERP/NYU/2014/SSC-01/002 to R.S.A.). The HiRAM simulations and analyses are carried out on the High Performance Computing resources of New York University Abu Dhabi. The HiRAM model is obtained from Geophysical Fluid Dynamics Laboratory, Princeton. The Program for Climate Model Diagnosis and Intercomparison is acknowledged for providing CMIP5 data.

- Sikka DR (1977) Some aspects of the life history, structure and movement of monsoon depressions. *Pure Appl Geophys* 115:1501–1529.
- Mooley DA, Shukla J (1987) Characteristics of the westward moving summer monsoon low pressure systems over the Indian region and their relationship with the monsoon rainfall (Center for Ocean-Land-Atmosphere Studies, George Mason Univ, Fairfax, VA), p 47.
- Krishnamurthy V, Ajayamohan RS (2010) Composite structure of monsoon low pressure systems and its relation to Indian rainfall. *J Clim* 23:4285–4305.
- Praveen V, Sandeep S, Ajayamohan RS (2015) On the relationship between mean monsoon precipitation and low pressure systems in climate model simulations. *J Clim* 28:5305–5324.
- Hurley JV, Boos WR (2015) A global climatology of monsoon low-pressure systems. *Quart J R Meteorol Soc* 141:1049–1064.
- Shukla J (1977) Barotropic-baroclinic instability of mean zonal wind during summer monsoon. *Pure Appl Geophys* 115:1449–1461.
- Boos WR, Hurley JV, Murthy VS (2015) Adiabatic westward drift of Indian monsoon depressions. *Quart J R Meteorol Soc* 141:1035–1048.
- Bollasina M, Ming Y, Ramaswamy V (2011) Anthropogenic aerosols and the weakening of the south Asian summer monsoon. *Science* 334:502–505.
- Krishnan R, et al. (2013) Will the south Asian monsoon overturning circulation stabilize any further? *Clim Dyn* 40:187–211.
- Rajeevan M, De US, Prasad RK (2000) Decadal variation of sea surface temperatures, cloudiness and monsoon depressions in the north Indian ocean. *Current Sci* 79:283–285.
- Dash SK, Kumar JR, Shekhar MS (2004) On the decreasing frequency of monsoon depressions over the Indian region. *Curr Sci* 86:1404–1411.
- Prajeesh AG, Ashok K, Rao DVB (2013) Falling monsoon depression frequency: A Gray-Sikka conditions perspective. *Sci Rep* 3:2989.
- Cohen NY, Boos WR (2014) Has the number of Indian summer monsoon depressions decreased over the last 30 years? *Geophys Res Lett* 41:7846–7853.
- Taylor KE, Stouffer RJ, Meehl GA (2011) An overview of CMIP5 and the experiment design. *Bull Am Meteorol Soc* 93:485–498.
- Zhao M, Held IM, Lin SJ, Vecchi GA (2009) Simulations of global hurricane climatology, interannual variability, and response to global warming using a 50-km resolution GCM. *J Clim* 22:6653–6678.
- Sabin TP, et al. (2013) High resolution simulation of the South Asian monsoon using a variable resolution global climate model. *Clim Dyn* 41:173–194.
- Ajayamohan RS, Merryfield WJ, Kharin VV (2010) Increasing trend of synoptic activity and its relationship with extreme rain events over central India. *J Clim* 23:1004–1013.
- Sikka DR (2006) A study on the monsoon low pressure systems over the Indian region and their relationship with drought and excess monsoon seasonal rainfall. Technical Report 217 (Center for Ocean-Land-Atmosphere Studies, George Mason Univ, Fairfax, VA), p 61.
- Ditchek SD, Boos WR, Camargo SJ, Tippet MK (2016) A genesis index for monsoon disturbances. *J Clim* 29:5189–5203.
- Cohen NY, Boos WR (2016) Perspectives on moist baroclinic instability: Implications for the growth of monsoon depressions. *J Atmos Sci* 73:1767–1788.
- Douglas MW (1992) Structure and dynamics of two monsoon depressions. Part I: Observed structure. *Mon Weather Rev* 120:1524–1547.
- Sandeep S, Ajayamohan RS (2015) Poleward shift in Indian summer monsoon low level jetstream under global warming. *Clim Dyn* 45:337–351.
- Held IM, Soden BJ (2006) Robust responses of hydrological cycle to global warming. *J Clim* 19:5686–5699.
- Krishnamurti TN, Molinari J, Pan H-L, Wong V (1977) Downstream amplification and formation of monsoon disturbances. *Mon Weather Rev* 105:1281–1297.
- Saha K, Sanders F, Shukla J (1981) Westward propagating predecessors of monsoon depressions. *Mon Weather Rev* 109:330–343.
- Knutson TR, et al. (2010) Tropical cyclones and climate change. *Nat Geosci* 3:157–163.
- Emanuel K, Sundarajan R, Williams J (2008) Hurricanes and global warming: Results from downscaling IPCC AR4 simulations. *Bull Am Meteorol Soc* 89:347–367.
- Ajayamohan RS, Rao SA (2008) Indian Ocean dipole modulates the number of extreme rainfall events over India in a warming environment. *J Meteorol Soc Jpn* 86:245–252.
- Goswami BN, Venugopal V, Sengupta D, Madhusoodanan MS, Xavier PK (2006) Increasing trend of extreme rain events over India in a warming environment. *Science* 314:1442–1445.
- Singh D, et al. (2014) Severe precipitation in northern India in June 2013: Causes, historical context, and changes in probability. [in “Explaining extremes of 2013 from a climate perspective”]. *Bull Amer Meteorol Soc* 95:558–561.
- Saha A, Ghosh S, Sahana AS, Rao EP (2014) Failure of CMIP5 climate models in simulating post-1950 decreasing trend of Indian monsoon. *Geophys Res Lett* 41:7323–7330.
- Krishnan R, et al. (2015) Deciphering the desiccation trend of the south Asian monsoon hydroclimate in a warming world. *Clim Dyn* 47:1007–1027.
- Turner AG, Annamalai H (2012) Climate change and the south Asian summer monsoon. *Nat Clim Change* 2:587–595.
- Tiwari VM, Wahr J, Swenson S (2009) Dwindling groundwater resources in northern India from satellite gravity observations. *Geophys Res Lett* 36, 10.1029/2009GL039401.
- United Nations, Department of Economic and Social Affairs, Population Division (2015) World population prospects: The 2015 revision, key findings and advance tables. Working Paper No. ESA/P/WP.241 (United Nations, New York).
- Levine RC, Turner AG, Marathayil D, Martin GM (2013) The role of northern Arabian Sea surface temperature biases in CMIP5 model simulations and future projections of Indian summer monsoon rainfall. *Clim Dyn* 41:155–172.
- Sandeep S, Ajayamohan RS (2014) Origin of cold bias over the Arabian Sea in climate models. *Sci Rep* 4:6403.
- Bruyère CL, Done JM, Holland GJ, Fredrick S (2013) Bias corrections of global models for regional climate simulations of high-impact weather. *Clim Dyn* 43:1847–1856.
- Rayner NA, et al. (2003) Global analyses of sea surface temperature, sea ice and night marine air temperature since the late nineteenth century. *J Geophys Res* 108: 4407.